European Journal of Pharmaceutical Sciences 143 (2020) 105151

Contents lists available at ScienceDirect

European Journal of Pharmaceutical Sciences

journal homepage: www.elsevier.com/locate/ejps

Essential role of STAT-3 dependent NF-κB activation on IL-6-mediated downregulation of hepatic transporters

Walaa A. Abualsunun, Cigdem Sahin, Carolyn L. Cummins, Micheline Piquette-Miller*

Department of Pharmaceutical Sciences, Leslie Dan Faculty of Pharmacy, University of Toronto, Toronto, ON, Canada

ARTICLE INFO

Keywords:
NF-κB
Inflammation
Transporters
Nuclear receptors
Il-6
PXR

ABSTRACT

IL-6 markedly decreases the expression of numerous hepatic transporters. We previously demonstrated that IL-6-mediated downregulation of transporters occurs through STAT3, with partial involvement of PXR. However, while IL-6-mediated induction of STAT3 occurs rapidly, repression of transporter expression is not observed until 6 h post-treatment. This temporal mismatch suggested that the downregulation of transporters following IL-6 at 6 h might require additional signaling downstream of STAT3. Since NF-κB has been implicated in endotoxin-mediated downregulation of transporters, we hypothesized that NF-κB may be similarly involved in suppressing transporter expression following IL-6. Our objective was to investigate whether IL-6-mediated changes in transporter expression occur through STAT3-dependent NF-κB activation, and whether PXR is involved. PXR null (-/-) or wild type (+/+) mice were pre-dosed with the NF-κB inhibitor PHA408 or vehicle 30 min prior to receiving a single dose of IL-6 or saline. Mice were euthanized after 6 h and transporter expression was analyzed using qRT-PCR. IL-6 imposed downregulation of *Abcb1a, Abcb1b, Abcc3, Abcg2* and *Cyp3a11* in both PXR (+/+) and PXR (-/-) mice, while downregulation of *Abcb11, Abcc2, Slc10a1*, and *Slco2b1* was only significant in PXR (+/+) mice. PHA408 pretreatment fully inhibited NF-κB activation in PXR (+/+) but only partially inhibited NF-κB in PXR (-/-). Inhibition of NF-κB attenuated IL-6-mediated changes in transporters in PXR (+/+) mice. Transient transfection assays did not detect significant activation of human or mouse PXR by PHA408. Our findings suggest that IL-6 imposes significant downregulation of numerous ABC and SLC transporters in the liver via collaborative STAT3/NF-κB activation. Since drug transporters play an integral role in the pharmacokinetics of numerous clinically relevant drugs, understanding the signaling pathways involved in transporter regulation during inflammation will contribute to a better understanding of drug-disease interactions.

1. Introduction

Circulating levels of the cytokine IL-6 play an important role in the hepatic regulation of several ATP-binding cassette (ABC) and solute carrier (SLC) transporters during acute inflammation (Merrell et al., 2014). Accumulating evidence shows that IL-6 administration down-regulates the expression of drug transporters, metabolizing enzymes and nuclear receptors including the pregnane X receptor (PXR) (Hartmann et al., 2002; Morgan et al., 2008; Evers et al., 2018). Previous studies have shown partial involvement of PXR in the IL-6-mediated downregulation of *Abcb11, Abcc2, Slco10a1* and *Slco2b1* (Teng and Piquette-Miller, 2005; Abualsunun and Piquette-Miller, 2018). However, the underlying regulatory mechanism of IL-6-mediated downregulation of hepatic transporters needs clarification. Although IL-6 modulation of gene transcription primarily occurs through the classical Janus Kinase/signal transducer and activator of transcription 3 (JAK/STAT3) signaling cascade (Moshage, 1997), other pathways may also be involved including MAP kinase (MAPK) and nuclear factor-kappaB (NF-κB) signaling pathways (Wang et al., 2003; Kishimoto, 2005). In an attempt to clarify the underlying regulatory mechanisms, our laboratory recently demonstrated that IL-6-mediated downregulation of hepatic transporters occurs largely via STAT3 activation (Abualsunun and Piquette-Miller, 2018). However, based on a time-dependent study that illustrated rapid activation of STAT3 following IL-6 administration along with immediate induction of hepatic transporters at early time points, we hypothesized possible involvement

Abbreviations: ABC,, ATP-binding cassette; CYP, cytochrome P450; NF-κB, nuclear factor kappa B; PXR, pregnane X receptor; SLC, solute carrier; Stat3, signal transducer and activator of transcription 3

* Corresponding author. Micheline Piquette-Miller, PhD., Professor, Leslie Dan Faculty of Pharmacy, University of Toronto, 144 College Street, Toronto, ON, M5S 3M2, Canada.

E-mail address: m.piquette.miller@utoronto.ca (M. Piquette-Miller).

https://doi.org/10.1016/j.ejps.2019.105151
Received 17 May 2019; Received in revised form 14 October 2019; Accepted 14 November 2019
Available online 15 November 2019
0928-0987/

of signaling pathways downstream of STAT3 activation in the ultimate IL-6-mediated downregulation of these transporters (Abualsunun and Piquette-Miller, 2018).

Activation of STAT3 rapidly induces expression of Suppressor of Cytokine Signaling-3 (*Socs3*), a STAT3/IL-6 target gene which triggers the release of secondary cytokines such as IL-1β and TNF-α, both of which are known to activate NF-κB. NF-κB is a transcription factor that regulates a plethora of genes involved in the inflammatory response, thereby playing a critical role in many diseases (Oeckinghaus and Ghosh, 2009). However, the transcriptional regulation of hepatic transporters following IL-6 administration has not been fully elucidated. We have previously demonstrated involvement of NF-κB in endotoxin-mediated downregulation of hepatic transporters (Abualsunun and Piquette-Miller, 2017). Of note, negative cross talk between NF-kB and PXR has been reported by several investigators (Gu et al., 2006; Xie and Tian, 2006; Zhou et al., 2006). Thus, our objective was to examine the role of NF-κB in IL-6-mediated regulation of hepatic transporters and determine whether PXR is involved.

2. Materials and methods

2.1. Animals and experimental design

C57BL/6 wild type [PXR (+/+)] mice purchased from Charles River Canada (Montreal, PQ, Canada) and PXR-deficient C57BL/6 [PXR (-/-)] mice, originally provided by Dr. Christopher Sinal (Dalhousie University, Halifax), were obtained from an inbred colony. Ten- to 12-week-old male PXR (+/+) and PXR (-/-) mice were administered a 40 mg/kg intraperitoneal (IP) injection of the selective NF-κB inhibitor PHA408 (Axon Medchem, Netherlands) or vehicle (dimethylsulfoxide/saline). Thirty minutes later, a single 1 μg IP dose of recombinant mouse protein IL-6 (R&D system, Minneapolis, MN) or saline was given. Mice (n = 5–8/group) were euthanized six hours after the second injection, and serum and livers were harvested, immediately frozen in liquid nitrogen and stored at −80 °C for further analysis. The PHA408 dose and timing of administration were based on previous *in vivo* studies conducted in rodents where it was shown that 40 mg/kg of PHA408 yielded a plasma concentration of 4 μM, which is well above the IC_{50} of the drug (40 nM) (Mbalaviele et al., 2009; Chiang et al., 2010; Rajendrasozhan et al., 2010). Furthermore, in our hands, this dose of PH408 effectively inhibited endotoxin-mediated NF-κB activation in mice (Abualsunun and Piquette-Miller, 2017). All animal studies were conducted in accordance with the guidelines of the University of Toronto Animal Care Committee and the Canadian Council on Animal Care.

2.2. Quantitative real-time polymerase chain reaction

The mRNA levels of each transporter were examined using qRT-PCR. Methods for RNA isolation, cDNA synthesis and qRT-PCR have been previously described (Abualsunun and Piquette-Miller, 2018). Briefly, RNA was extracted from liver tissues using the TRIzol method (Invitrogen, Carlsbad, CA) according to the manufacturer's instruction and reverse transcribed to single-stranded complementary DNA (cDNA) using a High Capacity cDNA RT kit (Applied Biosystems, Foster City, CA). Quantitative Real-time PCR was performed using the Power SYBR Green detection system (ABI HT 7900, Applied Biosystems, Streetsville, ON, Canada). The specific primer sequences used have been previously reported (Abualsunun and Piquette-Miller, 2017). The relative mRNA expression of each gene was calculated using the comparative Ct (ΔΔCt) method and each gene of interest was normalized to the housekeeping gene *36b4*. Normalization with 18S ribosomal RNA (*18S rRNA*) and glyceraldehyde-3-phosphate dehydrogenase (*Gapdh)* gave similar results.

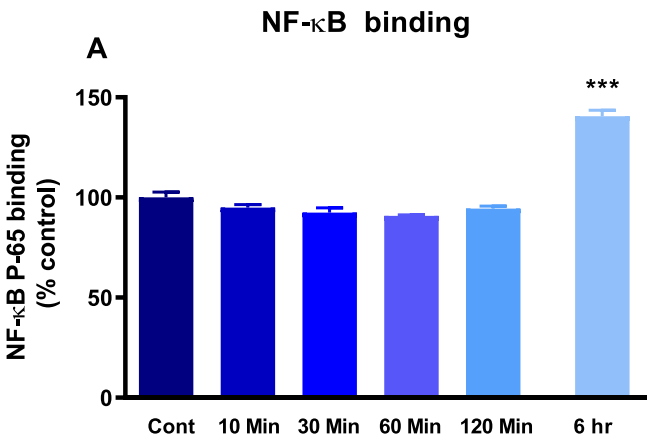

Fig. 1. Time course of NF-κB binding activity after administration of murine IL-6 in wild-type mice. NF-κB binding activity was measured in hepatic nuclear protein extracts by the NF-κB TransAM assay as described in methods. Data are presented as percentage of mean ± SD (n = 5–8). $^{***}P < 0.001$ significant from control (time zero).

2.3. Western blotting

Nuclear protein fractions were isolated from liver homogenates as previously described (Abualsunun and Piquette-Miller, 2017). The homogenates were centrifuged at 12,000 rpm for 10 min at 4 °C. Protein concentration was determined using the Bradford assay with BSA standards. Nuclear fraction lysates (40 μg) were denatured in Laemmli sample buffer (Biorad, Hercules, CA, USA) at 95 °C for 3 min, separated by 10% SDS-Polyacrylamide gel electrophoresis and then transferred to a polyvinylidene difluoride (PVDF) membrane (Bio-Rad Laboratories Canada, Mississauga, ON). Membranes were blocked with 5% skim milk in Tris-buffered saline with tween (TBST) and incubated overnight in 2% skim milk in TBST containing anti-PXR.1 primary antibody (A-20, 1:200, Santa Cruz Biotechnology) at 4 °C. Membranes were washed multiple times with TBST before incubation with anti-goat secondary antibody (1:3000, Jackson ImmunoResearch Laboratories, Inc., West Grove, PA). Immunodetectable levels were visualized and quantified with enhanced Super Signal West Pico Chemiluminescent Substrate (Thermo Scientific) and Alpha Ease FC imaging software (Alpha Innotech, Santa Clara, CA). β-actin (AC-15, 1:50,000, Sigma-Aldrich) was used as an internal control to normalize the uniformity of protein loading. The secondary antibody used to visualize β-actin was anti-mouse (1:5000, Jackson ImmunoResearch Laboratories, Inc.).

2.4. Transient transfection assays

In order to determine whether PHA408 activates PXR, CV-1 cells were transiently transfected with a GAL4-responsive reporter and plasmids encoding the ligand binding domains of mouse PXR (mPXR) or human PXR (hPXR) fused to the GAL4-DNA binding domain as previously described (Chan et al., 2013). GAL4-*hPXR*, GAL4-*mPXR* and UAS-luciferase (Firefly luciferase) were kindly provided by Dr. David Mangelsdorf (University of Texas Southwestern Medical Center, Dallas, TX). The pSL9-rLuc (*Renilla* luciferase) was kindly provided by Dr. Stephane Angers (University of Toronto, Toronto, ON). Briefly, CV-1 cells (derived from monkey kidney) were maintained in high-glucose Dulbecco's modified Eagle's medium (Invitrogen, Carlsbad, CA) supplemented with 10% FBS (37 °C in 5% CO_2). For transfection experiments, cells were seeded into 48-well plates in DMEM supplemented with 10% charcoal-stripped FBS. The following day, transfection was performed in OptiMEM media using Lipofectamine 3000 reagent (with a ratio of 1:2 of DNA to Lipofectamine 3000). The total amount of plasmid DNA (250 ng/well) included 125 ng UAS-*luciferase* reporter, 50 ng pSL9-*rLuc*, 50 ng GAL4-*mPXR/hPXR* and 25 ng of pGEM filler

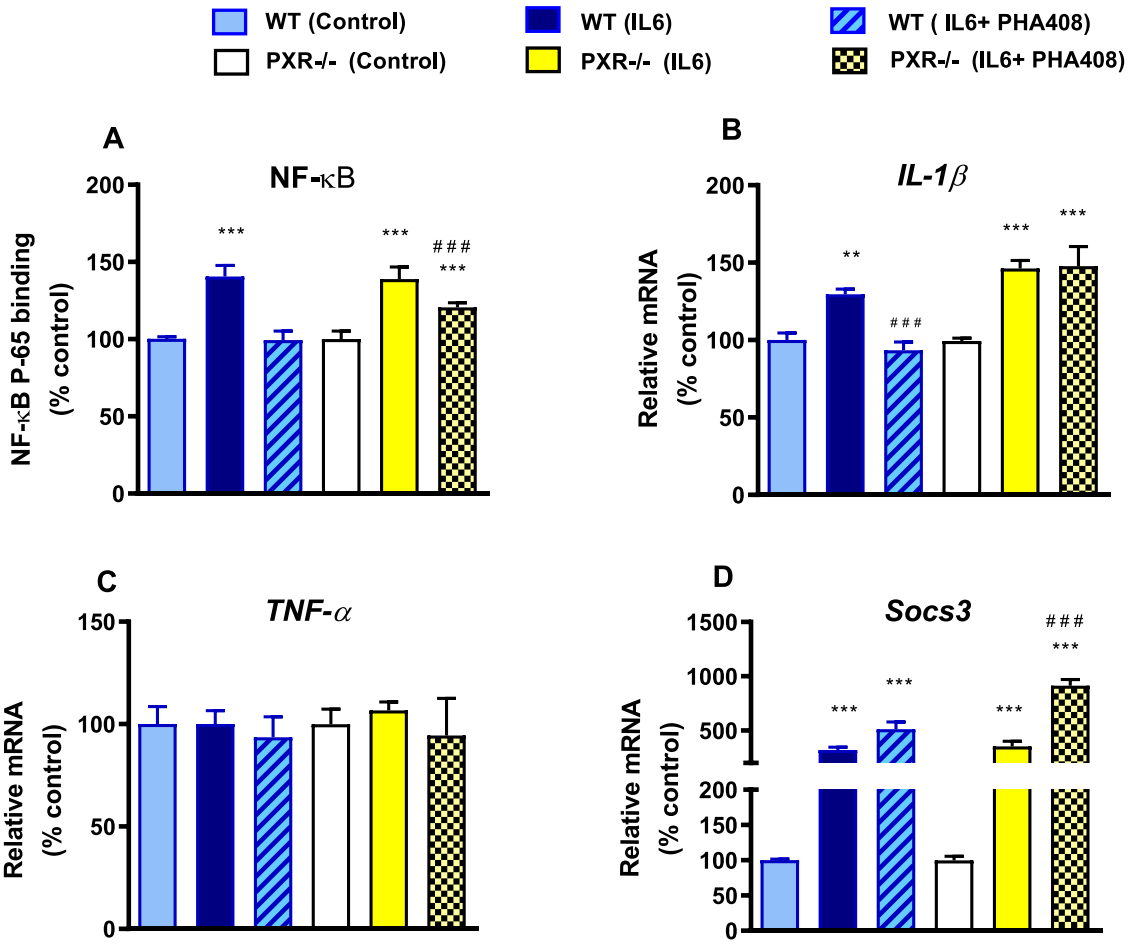

Fig. 2. Effect of IL-6 and PHA408 pretreatment on (A) NF-κB binding activity and hepatic mRNA levels of (B) *IL-1β*, (C) *TNF-α* and (D) *Socs3* (IL-6 target gene) in wild-type (WT) and PXR (-/-) mice at 6 h following murine IL-6 or saline (control) administration. NF-κB binding was measured in hepatic nuclear protein fractions by the TransAM assay while hepatic *TNF-α, IL-1β* and *Socs3* mRNA levels were measured by qRT-PCR, as described in methods. Data were normalized to saline controls and are presented as percentage of mean ± SD (n = 5–8). *Significant from controls, # significant from PXR WT. $^{**, \#\#}P<0.01$; $^{***, \#\#\#}P<0.001$.

plasmid. After 6 h, cells were then treated with vehicle (DMSO) or increasing concentrations of PHA408 (10 nM to 10 μM) in DMEM supplemented with 10% charcoal-stripped FBS. 10 μM 16α-carbonitrile (PCN) for *mPXR* and 10 μM SR12813 for *hPXR* were used as positive controls. Cells were harvested 16 h after ligand treatment and were lysed in 100 μl of lysis buffer (Promega), according to the manufacturer's instructions. Cellular lysate was assayed for firefly and *Renilla* luciferase activities using the Dual-Luciferase Reporter assay system (Promega). Firefly luciferase values were normalized to *Renilla* luciferase and expressed as normalized relative luciferase unit. Data from triplicate wells were averaged and expressed as mean ± SD.

2.5. Transcription factor DNA-binding (TransAM) assays

NFκB activation was measured using an NFκB TransAM kit (Active Motif, CA, USA) in accordance with the manufacturer's instructions. In this assay, the active form of NF-κB in the nuclear protein extract specifically binds to its target DNA (oligonucleotide that has been immobilized in the plate), and the primary antibodies used to detect NF-κB recognize an epitope that is accessible only when NF-κB is activated and bound to its target DNA. Using the kit, the specific DNA binding activity of NF-κB was measured in 4 μg of nuclear protein extract isolated from each liver sample. The absorbance was measured at 450 nm with a reference wavelength of 655 nm using a plate reader.

2.6. ELISA analysis

Levels of IL-6 were measured in serum collected from PXR (+/+) and PXR (-/-) mice six hours after administration of IL-6 or saline. Immunodetectable levels were measured according to the manufacturer's instructions using a commercially available mouse-specific enzyme-linked immunosorbent assay (ELISA) kit for IL-6 (R&D Systems, Minneapolis, MN). The minimum detectable limit was 1.3 pg/ml.

2.7. Statistics

Statistical analysis was performed using GraphPad Prism 7 software. Two-way ANOVA analyses were used to compare the mean differences between treatment groups followed by Tukey's multiple comparison tests to compare the means of all groups. Significance was defined as $P<0.05$. All results are expressed as mean ± standard deviation (SD).

3. Results

3.1. Effect of IL-6 and PHA-408 on inflammatory responses

Plasma concentrations of IL-6 were measured in order to establish the physiological relevance of the IL-6 dose used. IP administration of IL-6 yielded plasma concentrations of approximately 1100 ± 20 pg/ml in PXR (+/+) and 1250 ± 25 pg/ml in PXR (-/-) mice, which was not significantly different between the two strains. These plasma concentrations are consistent with IL-6 levels detected during an

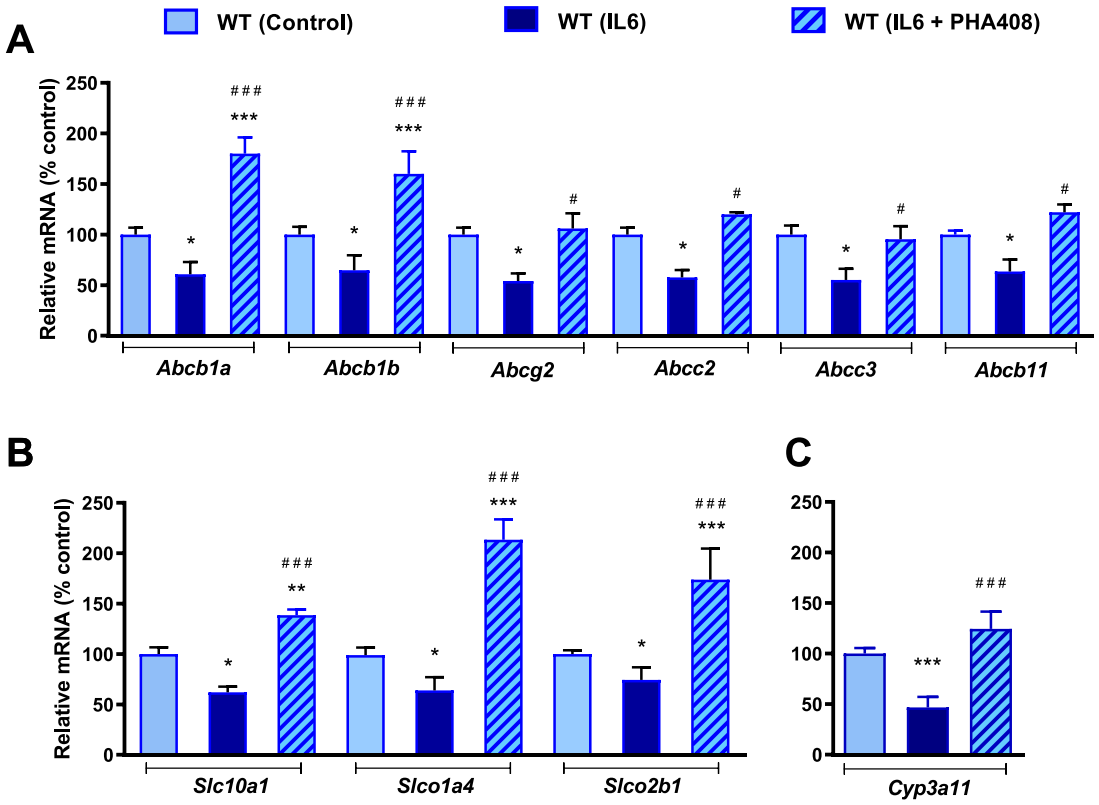

Fig. 3. Effect of PHA408 pretreatment on hepatic mRNA expression of (A) ABC (B) SLC transporters, and (C) ***Cyp3a11*** in wild type (WT) mice treated with IL-6 or saline (control) at 6 h. Data are normalized to PXR (+/+) [WT] controls and presented as percentage of mean ± SD (n = 5–8). * Significant from saline controls; # significant from IL-6 treated; $^{*,\#}P<0.05$; $^{**,\#\#}P<0.01$; $^{***,\#\#\#}P<0.001$.

endotoxemic inflammatory response in humans (≥1000 pg/ml) (Copeland et al., 2005).

NF-κB binding activity was investigated in order to examine whether IL-6 imposes an immediate or delayed activation of the NF-κB signaling pathway. We found that IL-6 administration did not significantly affect NF-κB binding to its target DNA at early time points (0–2 h), whereas NF-κB binding activity was increased at 6 h, indicating delayed activation of NF-κB signaling (Fig. 1). While similar increases in NF-κB binding activity were seen in both PXR strains, pre-treatment with the NF-κB inhibitor PHA408 was found to fully inhibit NF-κB activity in PXR (+/+) and partially inhibit NF-κB in PXR (-/-) mice (Fig. 2A). Basal levels of NF-κB binding were not different between PXR (+/+) and PXR (-/-) mice [102 ± 7% of PXR (+/+) control values].

To clarify the potential involvement of secondary cytokines in NF-κB activation, we measured mRNA levels of *IL-1β* and *TNF-α* at 6 h. While mRNA levels of IL-1β were increased in IL-6 treated PXR (+/+) and PXR (-/-) groups, pre-treatment with PHA408 attenuated mRNA levels in PXR (+/+) but not PXR (-/-) mice (Fig. 2B). *TNF-α* levels were not significantly changed in any treatment group (Fig. 2C). Following IL-6 administration, expression of the IL-6/STAT3 target gene, *Socs3*, was induced in both PXR (+/+) and PXR (-/-) mice, and induction was not affected by pre-treatment with PHA408 (Fig. 2D).

3.2. Effect of IL-6 and PHA408 on transporter expression

IL-6 administration suppressed the mRNA expression of several ABC and SLC transporters, including *Abcb1a, Abcb1b, Abcg2, Abcc2, Abcc3, Abcb11, Slco10a1, Slco1a4 and Slco2b1* as well as *Cyp3a11* in PXR (+/+) mice (Fig. 3). NF-kB inhibition via pretreatment with PHA408 effectively attenuated IL-6-mediated downregulation of these transporters. In PXR (-/-) mice, IL-6 administration also suppressed the mRNA expression of several transporters, including *Abcb1a, Abcb1b, Abcg2, Abcc3* and *Slco1a4* as well as *Cyp3a11* (Fig. 4). Since NF-κB was not effectively inhibited by PHA408 in PXR (-/-) mice, conclusions regarding the effect of NF-κB inhibition on IL-6-mediated changes in transporter expression could not be confirmed in the PXR (-/-) mice.

3.3. Effect of PHA408 on PXR expression and activation

To examine whether inhibition of NF-κB has an impact on the expression of PXR, transcript levels and nuclear protein levels of PXR were measured following IL-6 treatment in the presence or absence of PHA408. While significant decreases in the mRNA expression and nuclear protein levels of PXR were seen following IL-6 treatment, pre-treatment with PHA408 attenuated IL-6-mediated downregulation of PXR (Fig. 5).

To examine whether PHA408 increases transporter and PXR expression through PXR activation, we measured the effect of PHA408 on PXR activity using a transient transfection assay in CV-1 cells. The activity of mouse mPXR and human hPXR was measured after ligand treatment using a GAL4-responsive UAS-*luciferase* reporter. The positive controls PCN and SR12813, which are specific ligands for mPXR and hPXR, respectively, were used at a concentration of 10 μM. As expected, PCN and SR12813 induced two-fold and six-fold activation of mPXR and hPXR receptors, respectively. As compared to positive controls, PHA408 did not activate either mPXR or hPXR at concentrations of 1 – 50 μM (Figs. 6A, 6B). Taken together, these results show that PHA408 is not an activator of the PXR receptor.

4. Discussion

IL-6 modulates a vast number of genes through activation of the STAT3 signaling pathway. We recently demonstrated that inhibition of STAT3 attenuated IL-6-mediated downregulation of numerous hepatic

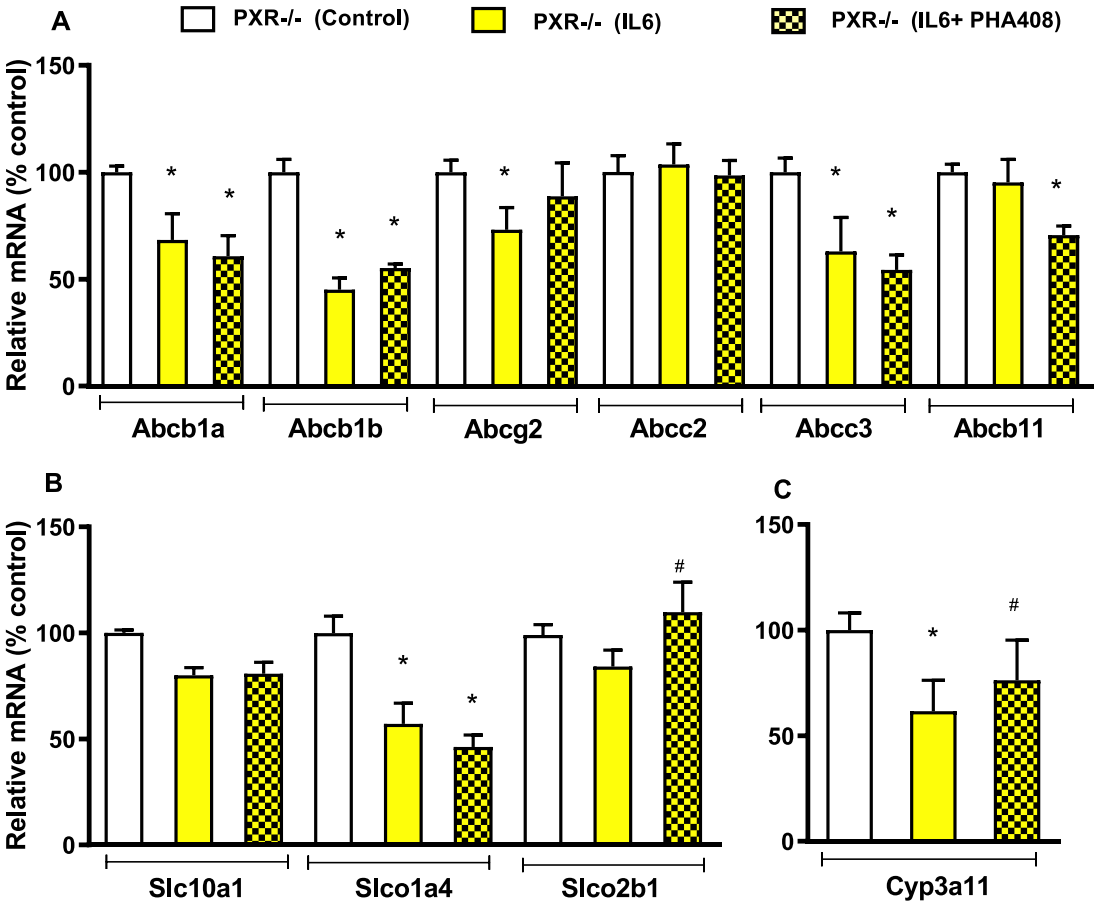

Fig. 4. Effect of PHA408 pretreatment on hepatic mRNA expression of (A) ABC (B) SLC transporters, and (C) ***Cyp3a11*** in PXR (-/-) mice treated with IL-6 or saline (control) at 6 h. Data are normalized to PXR (-/-) controls and presented as percentage of mean ± SD (n = 5–8). *Significant from saline controls, #significant from IL-6 treated; $^{*,\ \#}$ $P < 0.05$.

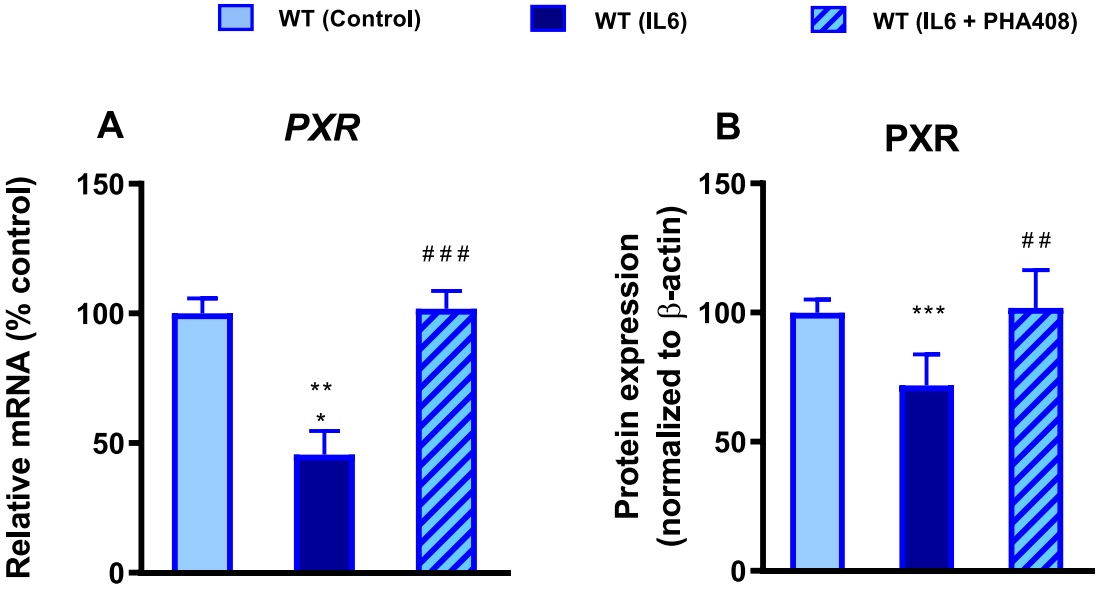

Fig. 5. Effect of PHA408 pretreatment on hepatic (A) mRNA and (B) nuclear protein expression of *PXR* in wild type (WT) mice treated with IL-6 or saline (Control)) at 6 h. mRNA and protein expression were determined as described in methods. Data are presented as percentage of mean ± SD (n = 5–8). * Significant from controls; and # significant from IL-6 treated. $^{**,\ \#\#}P < 0.01$; $^{***,\ \#\#\#}P < 0.001$.

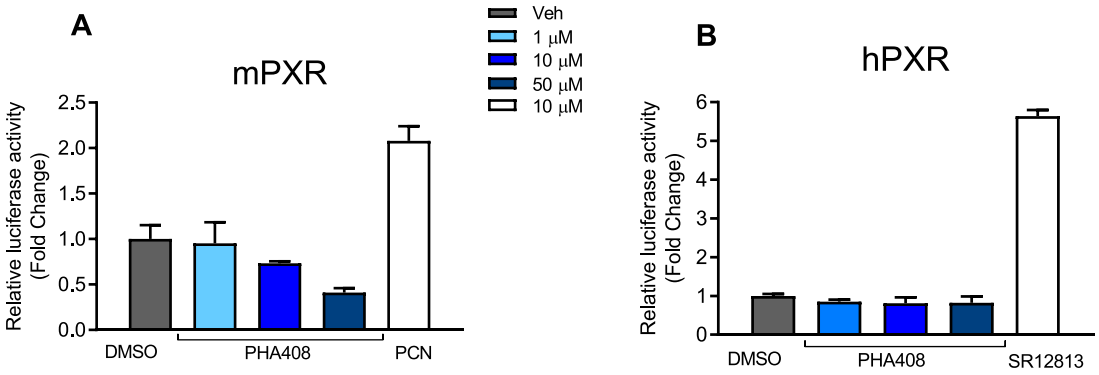

Fig. 6. Effect of PHA408 on mouse and human ***PXR*** promoter activity. CV-1 cells were transfected with plasmids expressing either (A) GAL4-mouse ***PXR*** or (B) GAL4-human ***PXR*** together with UAS-*luciferase* reporter plasmid. Transfected cells were treated with PHA408 at indicated concentrations for 16 hrs. PCN (10 μM) and SR12813 (10 μM) were used as positive controls for GAL4-***mPXR*** and GAL4-***hPXR***, respectively. Luciferase activities were measured as described in methods and normalized to *Renilla*. Results are expressed as fold induction versus vehicle. Data represent the mean ± SD (n = 3).

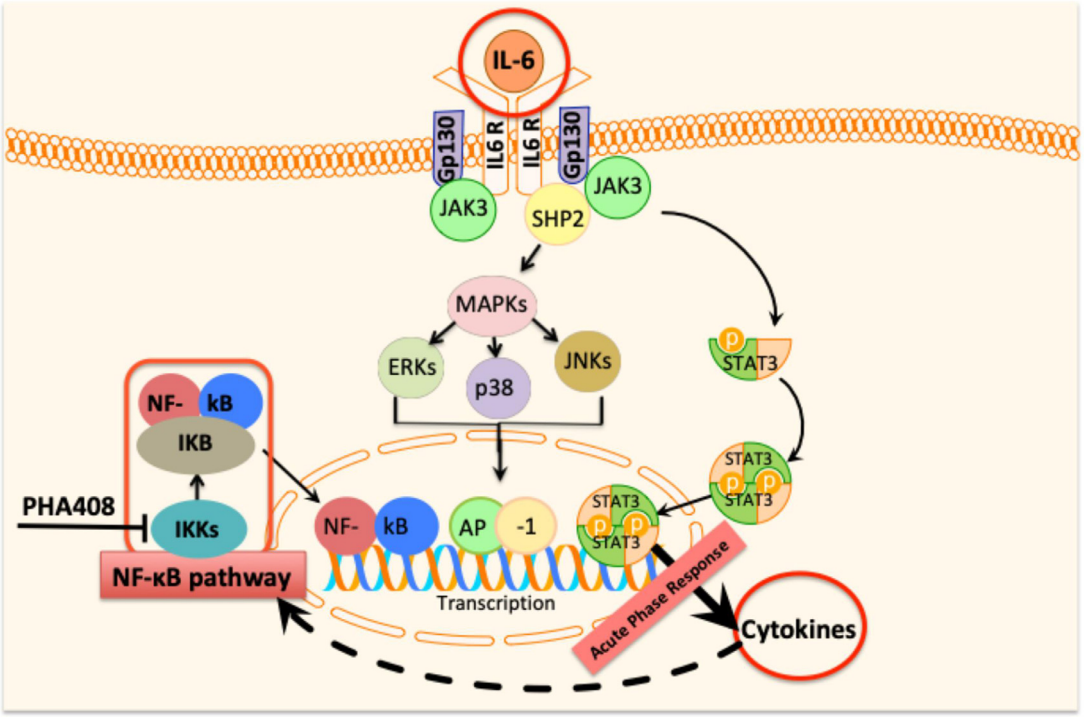

Fig. 7. Illustration of the IL-6/STAT3/NF-κB signaling pathways. IL-6 activates STAT3 phosphorylation and dimerization process allowing STAT3 to translocate into the nucleus where it activates the release of Socs3 and secondary cytokines. These secondary cytokines are known to activate the NF-κB signaling pathway.

transporters at 6 h. However, shortly after activation by IL-6, STAT3 was activated and transporter levels were induced (Abualsunun and Piquette-Miller, 2018). It is known that STAT3 activation increases production of pro-inflammatory cytokines such as IL-1β, which in turn activates the NF-kB signaling pathway. Thus, we hypothesized that IL-6-mediated downregulation of hepatic transporters may occur via STAT3 activation of NF-κB. Indeed, at six hours after IL-6 administration we observed *Socs3* and *IL-1β* induction and activation of NF-κB binding in both PXR (+/+) and PXR (-/-) mice (Fig. 2). Similar to previous reports (Teng and Piquette-Miller, 2005; Abualsunun and Piquette-Miller, 2018), significant decreases in the hepatic expression of numerous transporters were seen in the IL-6-treated mice at 6 h. Of particular importance, attenuation of these transporter changes were observed in PXR (+/+) mice that were pre-treated with the NF-κB inhibitor PHA408, indicating the involvement of NF-κB. The fact that NF-κB activation was only seen at 6 h and not at earlier time points suggests indirect activation of NF-κB, likely through STAT3 signaling. A summary of this proposed model is shown in Fig. 7.

PHA408 is a potent ATP-competitive inhibitor that selectively inhibits NF-κB signaling by tightly binding to the IKK-2 enzyme (Mbalaviele et al., 2009). Interestingly, we found that PHA408 pre-treatment fully inhibited NF-κB activation and transporter changes in PXR (+/+) mice but not in PXR (-/-) mice. It could be hypothesized that PXR (-/-) mice are less sensitive to NF-κB inhibition with PHA408. However, we previously demonstrated that similar doses of PHA408 fully inhibited NF-κB activation in both PXR (+/+) and PXR (-/-) mice after administration of endotoxin (Abualsunun and Piquette-Miller, 2017). Alternately, it is more likely that the discrepancy in inhibition seen between the two strains stem from differences in the pharmacokinetics rather than efficacy of PHA408. PHA408 is a positively charged molecule that is eliminated via hepatic clearance (Chiang et al., 2010). Dramatic 4 to 12-fold increases in basal expression levels of *Cyp3a11, Abcb1b, Abcc2* and *Abcg2* have been reported in the livers of PXR (-/-) mice (Staudinger et al., 2001; Gahir and Piquette-

Miller, 2011), which could lead to increased hepatic clearance of PHA408. Indeed, we previously reported higher hepatic clearances of lopinavir in PXR (-/-) as compared to PXR (+/+) mice (Gahir and Piquette-Miller, 2017). While PHA408 was effective at inhibiting endotoxin-mediated activation of NF-κB in PXR (-/-) mice, endotoxin is associated with very rapid NF-κB activation (within 20–40 min) (Abualsunun and Piquette-Miller, 2017). Since NF-κB activation was only seen 6 h after IL-6 administration (Fig. 1), systemic levels of PHA408 would be much lower at this time. Hence, differences in clearance could contribute to strain differences in PHA408 efficacy. As NF-κB activation was not fully inhibited in PXR (-/-) mice, we could not evaluate the potential contribution of PXR in IL-6/NF-κB mediated regulation.

We observed that the IL-6 mediated downregulation of PXR was attenuated by pretreatment with the NF-κB inhibitor, PHA408 (Fig. 5). Therefore, the observed increase in transporter expression after PHA408 could stem from restoration of PXR expression. However, we previously found that PHA408 pretreatment attenuated endotoxin-mediated downregulation of transporters in both PXR deficient and proficient strains (Abualsunun and Piquette-Miller, 2017), suggesting that restoration of PXR does not play a major role. The fact that we observed increased expression of several transporters in PHA408 + IL-6 treated PXR (+/+) but not PXR (-/-) mice suggested that PHA408 could be an activator of PXR. A pilot study in PHA408 treated mice detected increased *Abcg2* and *Cyp3a11* in PXR (+/+) but not PXR (-/-) mice (Supplementary data, Figure S1). However, many prototypical PXR target genes were not induced. Nevertheless, using a cell-based screening approach, we showed that PHA408 was not an activator of either mouse mPXR or human hPXR (Fig 5), indicating that PHA408 is not directly involved in PXR activation or the subsequent induction of PXR-regulated genes.

Altogether, this study demonstrates that IL-6-mediated downregulation of hepatic transporters occurs via signaling pathways downstream of STAT3 and that NF-κB activation is involved. IL-6-mediated activation of NF-κB likely occurs through STAT3-mediated induction of pro-inflammatory cytokines, which in turn activates NF-κB. The role of PXR in this mechanism remains unclear, as NF-κB was not sufficiently inhibited by PHA408 in the IL-6-treated PXR (-/-) mice. Further studies ensuring equivalent inhibitor exposure are needed. Since NF-κB is implicated in many diseases associated with inflammatory conditions, a better understanding of which signaling pathways are involved in regulating drug transporters may become a useful tool in treating and predicting potential drug-disease interactions.

Author contributions

Participated in research design: MPM, CLC and WAA.

Conducted experiments and data analysis: WAA (animal study, gene expression studies, NF-κB binding), CLC and CS (CV-1 cell transient transfection assay).

Performed data analysis: WAA.

Wrote or contributed to the writing of the manuscript: WAA, CS, CLC and MPM.

Acknowledgement

The authors thank Yen Ting Shen for his technical assistance.

Funding

Funding for this study was provided by an operating grant from the Canadian Institutes of Health Research [MOP 13346]. WA is a recipient of the King Abdul-Aziz University Scholarship for Postgraduate Studies.

Supplementary materials

Supplementary material associated with this article can be found, in the online version, at doi:10.1016/j.ejps.2019.105151.

References

Abualsunun, W.A., Piquette-Miller, M., 2017. Involvement of nuclear factor kappaB, not pregnane X receptor, in inflammation-mediated regulation of hepatic transporters. Drug Meta. Dispos. 45, 1077–1083.
Abualsunun, W.A., Piquette-Miller, M., 2018. STAT3 is involved in IL-6-Mediated downregulation of hepatic transporters in mice. J. Pharm. Sci. 21, 325s–334s.
Chan, G.N., Patel, R., Cummins, C.L., Bendayan, R., 2013. Induction of P-glycoprotein by antiretroviral drugs in human brain microvessel endothelial cells. Antimicrob. Agents Chemother. 57, 4481–4488.
Chiang, P.C., Kishore, N.N., Thompson, D.C., 2010. Combined use of pharmacokinetic modeling and a steady-state delivery approach allows early assessment of IkappaB kinase-2 (IKK-2) target safety and efficacy. J. Pharm. Sci. 99, 1278–1287.
Copeland, S., Warren, H.S., Lowry, S.F., Calvano, S.E., Remick, D., Inflammation, and the Host Response to Injury I, 2005. Acute inflammatory response to endotoxin in mice and humans. Clin. Diagn. Lab. Immunol. 12, 60–67.
Evers, R., Piquette-Miller, M., Polli, J.W., Russel, F.G.M., Sprowl, J.A., Tohyama, K., Ware, J.A., de Wildt, S.N., Xie, W., Brouwer, K.L.R., 2018. Disease-Associated changes in drug transporters may impact the pharmacokinetics and/or toxicity of drugs: A white paper from the international transporter consortium. Clin. Pharmacol. Ther. 104, 900–915.
Gahir, S.S., Piquette-Miller, M., 2011. Gestational and pregnane X receptor-mediated regulation of placental ATP-binding cassette drug transporters in mice. Drug Metab Dispos. 3, 465–471.
Gahir, S.S., Piquette-Miller, M., 2017. The role of PXR genotype and transporter expression in the placental transport of lopinavir in mice. Pharmaceutics 9, 49.
Gu, X., Ke, S., Liu, D., Sheng, T., Thomas, P.E., Rabson, A.B., Gallo, M.A., Xie, W., Tian, Y., 2006. Role of NF-κB in regulation of PXR-mediated gene expression: a mechanism for the suppression of cytochrome p-450 3A4 by pro-inflammatory agents. J. Biol. Chem. 281, 17882–17889.
Hartmann, G., Cheung, A.K., Piquette-Miller, M., 2002. Inflammatory cytokines, but not bile acids, regulate expression of murine hepatic anion transporters in endotoxemia. J. Pharmacol. Exp. Ther. 303, 273–281.
Kishimoto, T., 2005. Interleukin-6: from basic science to medicine–40 years in immunology. Annu. Rev. Immunol. 23, 1–21.
Mbalaviele, G., Sommers, C.D., Bonar, S.L., Mathialagan, S., Schindler, J.F., Guzova, J.A., Shaffer, A.F., Melton, M.A., Christine, L.J., Tripp, C.S., Chiang, P.C., Thompson, D.C., Hu, Y., Kishore, N., 2009. A novel, highly selective, tight binding IkappaB kinase-2 (IKK-2) inhibitor: a tool to correlate IKK-2 activity to the fate and functions of the components of the nuclear factor-kappaB pathway in arthritis-relevant cells and animal models. J. Pharmacol. Exp. Ther. 329, 14–25.
Merrell, M.D., Nyagode, B.A., Clarke, J.D., Cherrington, N.J., Morgan, E.T., 2014. Selective and cytokine-dependent regulation of hepatic transporters and bile acid homeostasis during infectious colitis in mice. Drug Metab. Dispos. 42, 596–602.
Morgan, E.T., Goralski, K.B., Piquette-Miller, M., Renton, K.W., Robertson, G.R., Chaluvadi, M.R., Charles, K.A., Clarke, S.J., Kacevska, M., Liddle, C., Richardson, T.A., Sharma, R., Sinal, C.J., 2008. Regulation of drug-metabolizing enzymes and transporters in infection, inflammation, and cancer. Drug Metab. Dispos. 36, 205–216.
Moshage, H., 1997. Cytokines and the hepatic acute phase response. J. Pathol. 181, 257–266.
Oeckinghaus, A., Ghosh, S., 2009. The NF-kappaB family of transcription factors and its regulation. Cold Spring Harb. Perspect. Biol. 1, a000034.
Rajendrasozhan, S., Hwang, J.W., Yao, H., Kishore, N., Rahman, I., 2010. Anti-inflammatory effect of a selective IkappaB kinase-beta inhibitor in rat lung in response to LPS and cigarette smoke. Pulmonary Pharmacology and Therapeutics 23, 172–181.
Staudinger, J.L., Goodwin, B., Jones, S.A., Hawkins-Brown, D., MacKenzie, K.I., LaTour, A., Liu, Y., Klaassen, C.D., Brown, K.K., Reinhard, J., Willson, T.M., Koller, B.H., Kliewer, S.A., 2001. The nuclear receptor PXR is a lithocholic acid sensor that protects against liver toxicity. Proc Natl Acad Sci USA 98, 3369–3374.
Teng, S., Piquette-Miller, M., 2005. The involvement of the pregnane X receptor in hepatic gene regulation during inflammation in mice. J. Pharmacol. Exp. Ther. 312, 841–848.
Wang, L., Walia, B., Evans, J., Gewirtz, A.T., Merlin, D., Sitaraman, S.V., 2003. IL-6 induces NF-kappa B activation in the intestinal epithelia. Journal of immunology 171, 3194–3201.
Xie, W., Tian, Y., 2006. Xenobiotic receptor meets NF-kB, a collision in the small bowel. Cell Metab. 4, 177–178.
Zhou, C., Tabb, M.M., Nelson, E.L., Grün, F., Verma, S., Sadatrafiei, A., Lin, M., Mallick, S., Forman, B.M., Thummel, K.E., et al., 2006. Mutual repression between steroid and xenobiotic receptor and NF-kB signaling pathways links xenobiotic metabolism and inflammation. J. Clin. Invest. 116, 2280–2289.